Environ Geol (2006) 49: 1089–1101
DOI 10.1007/s00254-005-0152-6

ORIGINAL ARTICLE

A. Navarro
H. Biester
J. L. Mendoza
E. Cardellach

# Mercury speciation and mobilization in contaminated soils of the Valle del Azogue Hg mine (SE, Spain)

Received: 8 March 2005
Accepted: 23 November 2005
Published online: 16 December 2005


A. Navarro (✉) · J. L. Mendoza
Dep. Mec. de Fluidos, Universidad Politécnica de Catalunya, ETSEIT, Colón 11, 08222 Terrassa, Spain
E-mail: navarro@mf.upc.es

H. Biester
Institute of Environmental Geochemistry, INF 236, 69120 Heidelberg, Germany

E. Cardellach
Dep. Geologia, Universitat Autónoma de Barcelona, 08193 Bellaterra, Spain

**Abstract** Hg mobilization from contaminated soils and mine wastes was the source of environmental contamination in the Valle del Azogue mining area. We researched solid-phase speciation and aqueous mobility of Hg through Scanning electron microscopy-energy dispersive X-ray spectroscopy and electron probe microanalysis analysis, solid-phase-Hg-thermo-desorption (SPTD) and laboratory column experiments. We found that in contaminated soils and mine wastes, the predominant Hg species was cinnabar (HgS), mainly formed from the weathering of Hg-rich pyrite, and metallic Hg (0) in the matrix, whereas in calcines and tailings the dominant species was metallic Hg (0). The mobilization of Hg in the aqueous phase seems to have originated from the dissolution of elemental Hg (0) present in soils and wastes, reaching concentrations of up to 67 μg $l^{-1}$, and showing a higher long-term environmental potential risk, in addition to atmospheric emissions.

**Keywords** Soil contamination · Calcines · Cinnabar

## Introduction

The Valle del Azogue mining area is located 100 km north–west of Almería, (Andalusia, SE Spain), in the prolongation of the Sierra Almagrera mining district (Fig. 1), which constitutes the central zone of the Cartagena-Cabo de Gata metallogenic belt (Navarro et al. 1994, 2004).

The Valle del Azogue mine was active approximately between 1873 and 1890. It was the main mercury mine in the Betic Cordillera producing about 1,000 t of Hg from two smelter sites located near the mining works. The only existing references to this deposit are by Cortazar (1875) and Becker (1888), who reported the presence of a Hg mineralization associated with exhalative deposits.

The mineralization consists of a set of small veins and breccias crosscutting the metamorphic host rocks from the Permian–Triassic age (phyllites and marbles from the Alpujárride complex) and occasionally overlying marls, sandy marls and limestones from the Tertiary age.

The mineral paragenesis comprises stibnite, cinnabar, As minerals (realgar and orpiment), sphalerite, siderite, chalcopyrite, pyrite, quartz, calcite and barite (Martínez et al. 1997). Hydrothermal and supergene alteration of primary minerals resulted in an association of secondary Fe/Mn and Sb–As oxides and hydroxides, kaolinite, jarosite and gypsum. The mineralized veins are characterized by high contents of Hg, Sb, As, Au, Ag, Pb, Zn and Ba (Table 1). Cinnabar occurs as disseminated grains of up to 1 mm, but generally $<100$ μm in siliceous breccia (see Fig. 4a), reaching grades of up to 1.3% by weight (Table 1).

The first environmental concerns about these old mines were reported by Martínez et al. (1998), Viladevall et al. (1999) and Navarro et al. (2000). Navarro et al. (2000) showed that the Hg vapour could have been released into the atmosphere through volatilization and transport by a Fickian mechanism of the metallic Hg (0) contained in the underground mineralization, soils and mine wastes (calcines, low ore stockpiles and slags). Moreover, the natural release of Hg into the atmosphere facilitated a near-surface deposition of Hg (0) in soils and sediments, which was added to the Hg (0) accumulated from the furnaces operating during the ninetieth century.

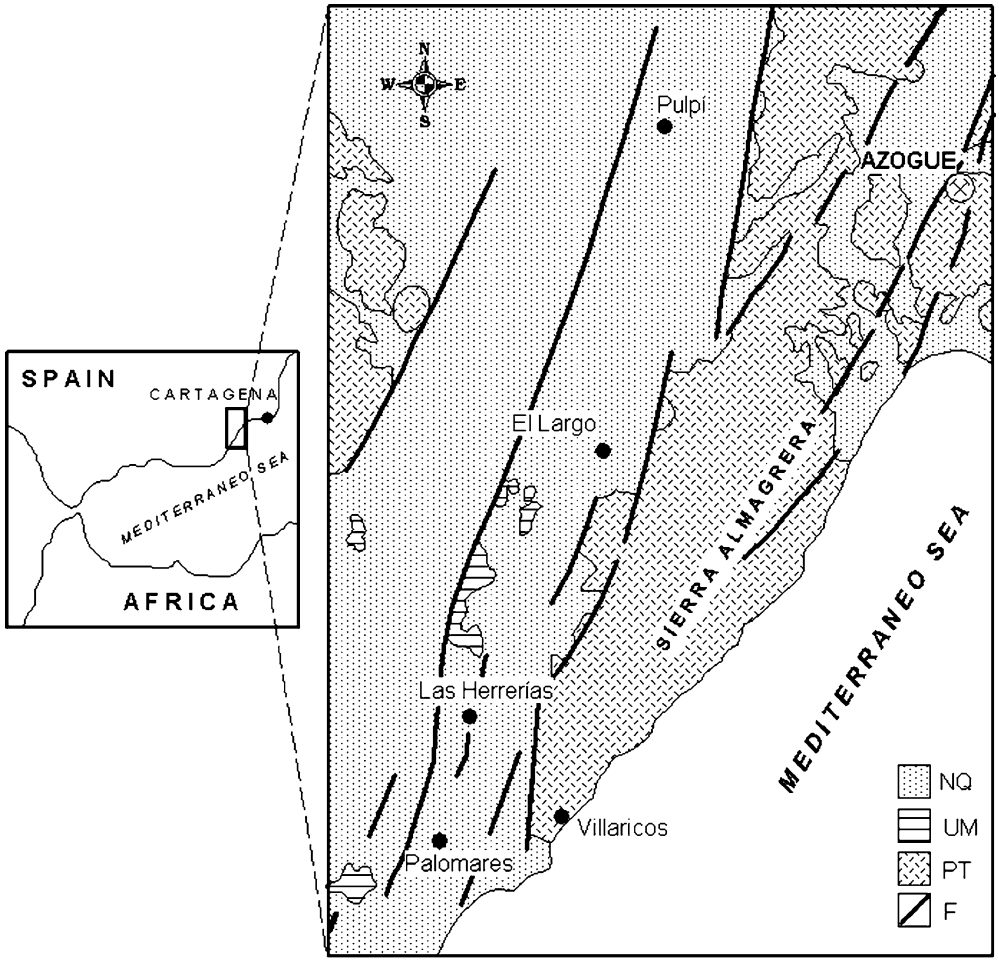


**Fig. 1** Situation map (*inset*) and synthetic Geology of the study area. *NQ* Neogene-Quaternary, *UM* volcanic–shoshonitic rocks, *PT* metamorfic basament, *F* main faults

Mercury ores were processed in retorts, producing coarse-grained, poorly sorted calcines, and placed near the furnace in small stockpiles.

A preliminary geochemical characterization of soils (Table 2) indicated a contaminated area with mean Hg values of 357.3 mg $kg^{-1}$ and significantly high amounts of As (mean 353.9 mg $kg^{-1}$), Sb (mean 3,117 mg $kg^{-1}$), Au (mean 49 μg $kg^{-1}$), Ag (mean 8.4 mg $kg^{-1}$), Pb (mean 361 mg $kg^{-1}$), Zn (mean 535 mg $kg^{-1}$) and Ba (mean 16,117 mg $kg^{-1}$). As and Hg occurred as trace elements in pyrite and as small realgar–orpiment prismatic crystals, possibly of secondary origin, disseminated in the breccia (see below).

The environmental impact of mining had a strong effect on vegetation. Hg contents of between 10–20 mg $kg^{-1}$ in "thyme plants" and up to 100 mg $kg^{-1}$ in pepper were found in the agricultural area near the mining site (Viladevall et al. 1999).

The mobilization of contaminants by mechanical dispersion, volatilization (Hg), and surface waters resulted in the region's main concentration of contamination from old mines.

**Table 1** Geochemical characteristics of mineralization in the Azogue Mining Area

| Element | Mean | St. Deviation | Max. | Min. | Phylites |
|---|---|---|---|---|---|
| Hg | 13,380.5 | 32,039.8 | 110,000 | 1 | < 1 |
| Sb | 14,773.4 | 27,232.1 | 96,000 | 7.5 | 3.8 |
| As | 393.7 | 333.9 | 1,200 | 19 | 50.8 |
| Au | 164 | 250.8 | 823 | 5 | 2 |
| Ag | 23.6 | 43.8 | 160 | 5 | < 0.3 |
| Pb | 67.2 | 105.5 | 276 | 2 | 47 |
| Zn | 555.8 | 464.3 | 2,705 | 50 | 123 |
| Ba | 52,096 | 110,118.2 | 390,010 | 200 | 460 |

Values in mg $kg^{-1}$ and Au (μϖ g $kg^{-1}$). Determinations by INAA and ICP-MS (Ag, Pb and Zn)

**Table 2** Main geochemical characteristics of contaminated soils in the Azogue Mining Area

| Element | Mean | St. Deviation | Max. | Min. | NCS |
|---|---|---|---|---|---|
| Hg | 357.3 | 587.7 | 2,300 | 1 | < 1 |
| Sb | 3,117.7 | 6,829.3 | 32,000 | 19 | 22 |
| As | 353.9 | 399.6 | 1,610 | 18 | 18 |
| Au | 49.0 | 98.6 | 480 | 5 | < 5 |
| Ag | 8.4 | 11.6 | 60 | 5 | < 5 |
| Pb | 361.4 | 601.7 | 2,554.9 | 7 | 15 |
| Zn | 535.1 | 755.8 | 2,970 | 50 | 90 |
| Ba | 16,117 | 32,264.6 | 170,000 | 200 | 870 |

Values in mg $kg^{-1}$ and Au (μϖ g $kg^{-1}$). Determinations by INAA and ICP-MS (Ag, Pb and Zn)*NCS* Non contaminated soils

This paper aims to characterize the solid phases of Hg present in the ore, soil, calcines and mine wastes, and to evaluate the mobility of Hg in the aqueous phase. Solid-phase Hg speciation is important for determining the risk of contaminated soils and wastes, because the environmental risk posed by Hg is directly related to its environmental mobility (Barnett et al. 1997, Rytuba 2002).

Previous studies showed that Hg pyrolysis is a useful technique for distinguishing cinnabar from metallic Hg (0) or matrix-bound Hg (Biester and Scholz 1997; Biester et al. 1999). In order to better characterize the Hg-bearing species in soils, calcines and ore samples, Hg pyrolysis data were complemented with SEM-EDS and EPMA analyses. Finally, the mobilization of Hg in aqueous phase was determined by column experiments, using the PHREEQC model to evaluate the mass transfer between the soil and the pore water flowing through the column.

## Materials and methods

### Soil characterization

Samples of soils and mine wastes were collected and analysed to determine the concentration of mercury and other trace elements, and to evaluate their speciation and aqueous mobility. Soils and sediments were hand-sampled using a method derived from standardized methods for describing and sampling contaminated soils (EPA 1991). The metal contamination and composition of the soils was determined using local geochemical profiling from soil cores sampled in areas of apparently high contamination. We obtained 80-cm-deep soil cores from auger holes and stainless steel soil sample rings, taking four samples from each core at 20 cm intervals.

The soil, sediment and tailing samples were sealed to minimize exposure to the atmosphere and dried them at 30°C for 48 h. Soil and mine wastes were then homogenized and their grain size, porosity and bulk density was determined. In the samples from soil profiles grain size, porosity, bulk density, pH and electric conductivity were measured.

Before carrying out the chemical analysis, we powdered and homogenized the soil, calcines and mining wastes. We quantitatively analysed Au, Ag, As, Ba, Br, Ca, Ce, Co, Cr, Cs, Eu, Fe, Hf, Hg, Ir, La, Lu, Na, Ni, Nd, Rb, Sb, Sc, Se, Sm, Sn, Sr, Ta, Th, Tb, U, W, Y and Yb by instrumental neutron activation analysis (INAA) and Mo, Cu, Pb, Zn, Ag, Ni, Mn, Sr, Cd, Bi, V, Ca, P, Mg, Tl, Al, K, Y and Be by inductively coupled plasma emission spectroscopy (ICP-OES). Table 3 shows the results of these analyses.

We also analysed ore samples to discover the mean metal contents of the ore deposit and their influence on the Hg species in the soil, calcines and mining wastes. Table 4 shows the results.

**Table 3** Geochemistry of soils and mine wastes used in the study of speciation and aqueous mobility

| Sample | Description | Hg | Sb | As | Au | Ag | Pb | Zn | Ba |
|---|---|---|---|---|---|---|---|---|---|
| M02 | Soil | 450 | 1,300 | 296 | 30 | 13 | 670 | 549 | 19,000 |
| M03 | Calcine | 470 | 14,800 | 1,610 | < 76 | 75.1 | 2,555 | 2,002 | 170,000 |
| A01 | Mine waste | 530 | 1,200 | 300 | 23 | 9.6 | 489 | 336 | 75,000 |
| A02 | Mine waste | 1,000 | 1,800 | 620 | 32 | 24.6 | 1,497 | 4,033 | 58,000 |
| A03 | Soil | 210 | 625 | 184 | 7 | 3.1 | 323 | 543 | 29,000 |
| A04 | Mine waste | 540 | 8,600 | 680 | < 164 | 108.7 | 3,422 | 14,295 | 170,000 |
| A05 | Calcine | 400 | 4,200 | 320 | 66 | 39.3 | 1,143 | 878 | 100,000 |
| A06 | Mine waste | 600 | 2,200 | 610 | < 35 | 9.7 | 778 | 2,074 | 17,000 |
| A07 | Mine waste | 820 | 2,600 | 410 | < 43 | 21.3 | 799 | 954 | 38,000 |

Values in mg $kg^{-1}$ and μg $kg^{-1}$ (Au)

**Table 4** Geochemistry of ore samples used in the study of speciation

| Sample | Description | Hg | Sb | As | Au | Ag | Pb | Zn | Ba |
|---|---|---|---|---|---|---|---|---|---|
| M04 | As rich ore | 77 | 27,500 | 718 | 183 | 55 | 101 | 226 | 210,000 |
| A08 | Sb rich ore | 220 | 96,000 | 26 | 240 | 5.4 | 2 | 1,047 | 28,000 |
| A09 | Hg rich ore | 110,000 | 1,400 | 36 | 26 | 0.8 | 12 | 2,705 | 96,000 |
| B01[a] | Calcine | 66 | 6.0 | 9.6 | 9 | < 0.3 | 20 | 77 | 380 |
| B04[a] | Cinnabar ore | 4,600 | 34.4 | 5.1 | 2 | < 5 | 31 | 93 | < 50 |

Values in mg $kg^{-1}$ and μg $kg^{-1}$ (Au)
[a]Samples obtained in the near Hg mining of Bayarque (silica-carbonate hosted Hg mineralization)

Hg, Sb, As, Au, Ag, Pb, Zn and Ba concentrations in soil, calcines and mining wastes were high and similar to the values previously published by Navarro et al. (2000).

Although the mercury content in the soils and mine wastes ranged from 357 to 1,000 mg $kg^{-1}$, the concentration in calcines was especially remarkable (66–470 mg $kg^{-1}$), above the mean values reported by Rytuba (2000) for calcined tailings from rotary furnaces (20–150 mg $kg^{-1}$), and similar to those of calcined tailings from Scott furnaces (500–1,000 mg $kg^{-1}$, Rytuba 2000) and tailing samples from the Idrija mercury mine (42–1,640 mg $kg^{-1}$, Biester et al. 1999). The evolution of contaminants in the soil profiles from the central area of the Valle del Azogue mine (Fig. 2) showed a decrease in Hg and As concentrations with depth, suggesting a similar evolution of As and Hg in the soil and a possible enrichment in Pb with depth associated with the likely presence of base metals in the deeper sections of the mineralization.

## Soil mineralogy

The mineralogy of the soil samples was examined under a binocular microscope and the fine fraction was analysed using X-ray powder diffraction (XRD). The results of the mineralogical study indicated that the most abundant minerals were quartz (80–85%), mica (5–10%), feldspar (5–10%), barite (1–5%), calcite (1–5%), and hematite (1–5%), while the secondary minerals were jarosite ($KFe_3(SO_4)_2(OH)_6$), crystalline oxyhydroxide of Fe (goethite), amorphous ferric hydroxide ($Fe(OH)_3$), clay minerals and gypsum ($CaSO_4{\cdot}2H_2O$).

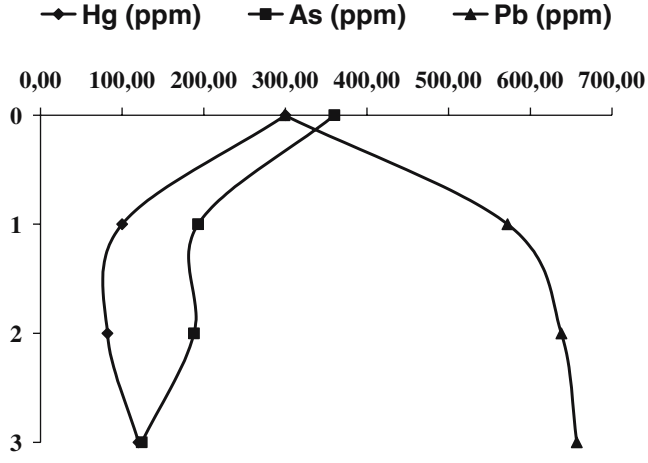


**Fig. 2** Evolution of Hg, As and Pb in a soil profile of the Valle del Azogue mine. *Sample 0* 0–0.1 m, *sample 1* 0.1–0.27 m, *sample 2* 0.27–0.51 m, *sample 3* 0.51–0.8 m

## Major and trace element analysis of minerals

Scanning electron microscopy (SEM) and energy dispersive X-ray spectroscopy (EDS) were used to characterize the solid forms of Hg in ore, soil and calcine samples at the Electronic Microscopy Laboratory of the Autonomous University of Barcelona. Pyrite was quantitatively analysed using electron probe microanalysis (EPMA) to determine the presence of Hg, Ni, Co, Sb and As in this mineral using a Cameca SX50 at the Analysis Services of the University of Barcelona. We obtained quantitative data by comparing the intensities of X-rays generated from the sample with standards of known composition. In this case, we used the following compounds as standards: HgS, $FeS_2$, InSb, GaAs, NiO and Co. The working conditions were 20 Kv and 20 nA with 10 s of acquisition time for each element.

## Thermo-desorption analysis of Hg

The determination of Hg phases by solid-phase-Hg-thermo-desorption (SPTD) is based on the specific thermal desorption or decomposition of Hg compounds from solids at different temperatures. SPTD can identify fewer species than other methods (EXAFS), but it is a good method for identifying Hg (0) and solid matrix with elemental mercury (Sladek et al. 2002).

We determined the mercury thermo-desorption curves using an in-house apparatus consisting of an electronically controlled heating unit and an Hg-detection unit. For Hg detection, we placed a quartz cuvette, through which the thermally released Hg is purged in the optical system of an atomic absorption spectrometer

(Perkin-Elmer AAS 3030) and detected absorption at 253.7 nm in continuous-detection mode (1 s intervals). Interferences, mainly from pyrolysis products of organic matter, were compensated by means of continuous deuterium background correction. Measurements were carried out at a heating rate of 0.5°C $s^{-1}$ and nitrogen-gas flow of 300 ml $min^{-1}$. The sample weight was 1–20 mg depending on the Hg content of the sample. The lowest level of detection under the given conditions is in the range 40–50 ng if all Hg is released within a single peak (Biester and Scholz 1997). Figure 3a–c depict the results as Hg thermo-desorption curves (Hg-TDC) which show the release of Hg (0) versus temperature.

### Laboratory column experiments

In order to evaluate the aqueous mobility of Hg and related metals, we carried out a laboratory column-leaching experiment. The experiment was conducted in a controlled environment using a sample of contaminated soil (M02, see Table 3), that contained 450 mg $kg^{-1}$ of total Hg, mainly as metallic Hg (0) as indicated by the thermal analysis (Fig. 3a). The column-leaching experiments allow us to obtain, a collection of "pore waters" produced by the percolation of demineralized water through the contaminated soil.

The experimental setup consisted of a reservoir with demineralized water, a transparent column with an internal diameter of 150 mm and a length of 750 mm, and a titration pump. The column was uniformly packed with the contaminated soil between two layers of very low reactivity polystyrene particles with an equivalent diameter of 2.97 mm. The demineralized water was introduced into the column using a "rain-simulator", which was connected to a titration pump that supplied a mean flow rate of 2.72 l $h^{-1}$. The column's dimensions were designed to minimize the occurrence of channelling because its diameter is at least 30 times the maximum particle size found in the material used (Relyea 1982). The column column's length (750 mm) was four times its diameter (150 mm), thereby fulfilling the minimum length-to-diameter ratio requirements for this type of experiment (Relyea 1982).

A plastic funnel that was 222 mm long and had an inner diameter of 186 mm was attached to the lower part of the column and a perforated fibreglass plate was installed inside the funnel to support the column's methacrylate structure. The plate was covered by a mesh that acted as a filter and retained the porous medium. The entire device was mounted on top of a metal structure that allowed its height above the surface and the verticality of the column to be regulated.

The leachates were collected at the bottom of the column as a function of time. The first sample was taken when water started to flow from the lower part of the column. Flow, Eh, pH, $O_2$ and conductivity were measured immediately after sample collection. The concentrations of cations, metals and rare elements were determined after acidification (using ultrapure $HNO_3$) of up to pH = 1.5 by ICP-OES. Chloride, nitrate, nitrite, fluoride, bromide, phosphate and sulphate were analysed on an aliquot of untreated sample using ion chromatography.

The PHREEQC geochemical code (Parkhurst and Appelo 1999) was used for the inverse modelling between the soil pore water and the demineralized water used in the experiment column. Inverse modelling in the PHREEQC code is a geochemical mole-balance model that locates sets of minerals and gases that, when reacted in the appropriate amounts, describe the mass transfer and the hydrogeochemical changes between up-flowing and down-flowing waters and can explain the results of a column experiment. In the inverse modelling applied, the Minteq thermodynamic database was used for the chemical equilibrium calculations.

## Results and discussion

### SEM-EDS and EPMA study

Optical and textural studies on polished sections of ore samples confirmed that stibnite is the most abundant primary sulphide. It developed needle-like crystals and was accompanied by minor amounts of sphalerite, pyrite, cinnabar and barite. Cinnabar was the only optically recognized Hg-bearing mineral. It was present as powder-like concentrations scattered in soil and ore samples, frequently coating barite, pyrite, quartz and carbonate crystals (Fig. 4a, b). In terms of texture, cinnabar was the last mineral to precipitate and tended to be found in association with Sb secondary minerals (cervantite, stibiconite and valentinite).

The presence of metallic Hg was exceptional and restricted to samples from calcines, where metallic Hg particles were found filling voids or coating silicate crystals. The presence of cinnabar particles in soils (Fig. 4b) and metallic Hg (0) in calcines was in accordance with the geochemical vapour surveys and pyrolysis determinations.

The textures and spatial distribution in the ore and soil samples suggested that the cinnabar had formed through the weathering of a primary Hg-bearing phase, probably pyrite. In order to check this hypothesis, we performed a quantitative analysis of minor and trace elements in pyrite. Table 5 shows the results as elemental weight percent.

The analytical results showed that Hg, Sb and As contents in pyrite were very high. Hg ranged from 0.12 to 0.88%, Sb from 0.12 to 1.6% and As from 0.53 to 1.53%.

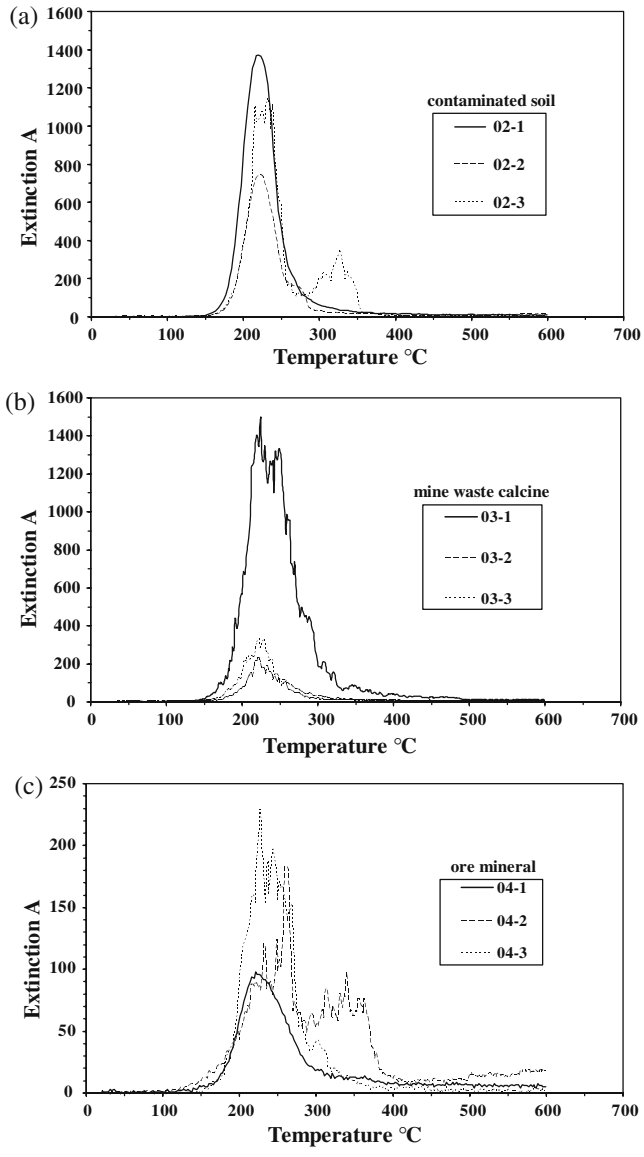


**Fig. 3** Mercury thermo-desorption curves of soil sample M02 (**a**), calcine M03 (**b**) and As rich ore M04 (**c**)

The high concentration of Hg (up to 8,800 mg $kg^{-1}$) was especially significant, as it could explain the presence of powder-like cinnabar associated with Fe oxides and hydroxides resulting from the oxidation of pyrite (see Fig. 4a). The cinnabar would then be the result of supergene alteration of pyrite and would tend to concentrate in soils and altered ores. This hypothesis is supported by the presence of cinnabar crystals coating microscopic cavities, usually associated with the Sb and As secondary minerals. The trace metal analysis of soils also showed a decrease in the Hg content with depth (see Fig. 2), which would be expected in weathered soil profiles, in which the degree of soil alteration decreases with depth.

## Thermo-desorption measurements

Hg was released from samples (Fig. 3a–c) at two different temperature ranges 220–250 and 310–330°C. Because the temperature of metallic Hg liberation in this type of experiment is about 100°C (Biester et al. 1999), we can conclude that no "free metallic Hg" was present in the soils and wastes analysed by thermo-desorption. According to Biester et al. (1999), the first peak indicates Hg released from the matrix, whereas the second peak at higher temperatures indicates the occurrence of cinnabar. Thus, our data showed that cinnabar was always present in the soil and ore samples and almost absent in calcines with the exception of the B01 sample.

This Hg release pattern was usually found in calcinated samples. During roasting, most of the cinnabar decomposed, releasing $SO_2$ and Hg vapour, but some Hg was readsorbed into the calcinated material during cooling. In soils (M02, A03) and mine-waste samples composed of host rocks and low-grade ore (A01, A02 samples), we detected Hg (0) and cinnabar. In ore samples, we recognized cinnabar and a possible Hg-sulphate.

Samples M02 (Fig. 3a), M03 (Fig. 3b), A01–A07 (Fig. 5a–g) and B01 (Fig. 5h) show the Hg-TDCs of soil, mine waste, tailing and calcine samples. The results show a predominant release of Hg in the temperature range of 200–300°C with a maximum release between 220 and 250°C. According to the Hg-TDCs of standard materials, this temperature range was assigned to the release of Hg from soil matrix components.

Unlike natural soils, calcines and tailings in the sampled area were free of organic matter, which is known to have a high capacity for Hg binding. Thus, we assume that most Hg in tailings is bound to mineral components. A previous study found that Hg (0) that formed during the thermal breakdown of cinnabar recondensed during cooling and adsorbed into dehydrated iron oxide surfaces (Biester et al. 1999). Sample B01, taken directly from the furnace outlet (Fig. 5h) and sample M02 (Fig. 3a) showed the same Hg release features as tailing samples. This suggests that the matrix-bound Hg found in tailings is mainly formed during the roasting process and that the atmospheric deposition of Hg (0) derived from roasting-plant emissions was of minor importance. Clay minerals, mainly kaolinite, which are also present in the tailings showed a much lower capacity to bind Hg. Free metallic Hg which is typically released at temperatures below 100°C could not be detected in any of the analysed samples. The presence of cinnabar in some calcine samples (B01, Fig. 6h) could be the result of an incomplete breakdown of the ore during the roasting process.

We found cinnabar to be the predominant form of Hg in some of the unprocessed ore samples, as

indicated by the Hg release curves in Fig. 6b (sample A09) and 6d (sample B04). Since cinnabar was found to be the predominant form of Hg, as in some of the mine wastes we assumed that this was the unprocessed/roasted material.

We also found cinnabar to be the predominant geogenic Hg species in alluvial soils in the study area (sample M02 in Fig. 3a and sample A03 in Fig. 5c), although we also detected matrix-bound Hg forms in all of the unprocessed samples as well.

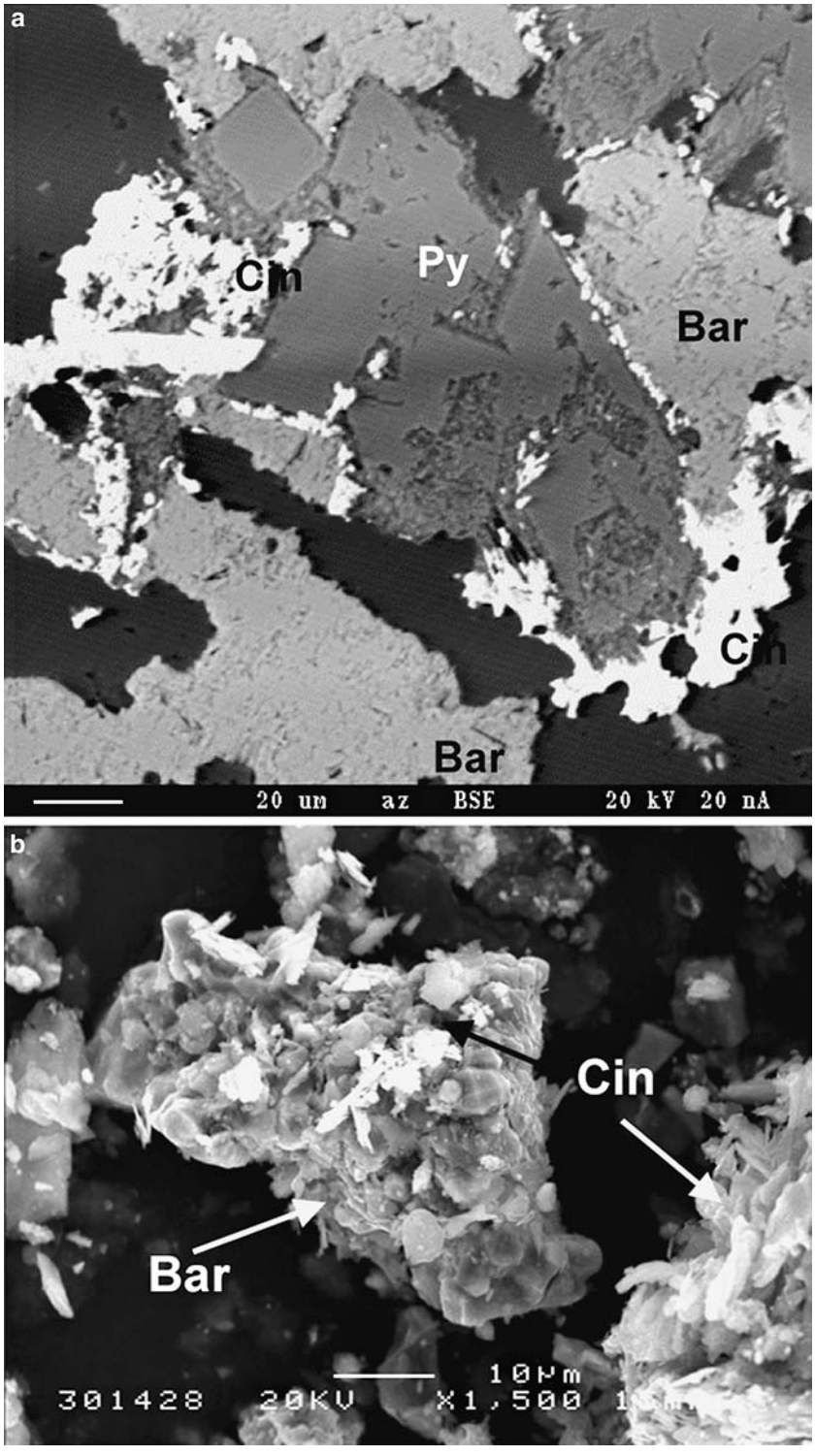


**Fig. 4** **a** Pyrite crystal (*Py*) surrounded by secondary cinnabar (*Cin*) and barite (*Bar*). BSE image. *Scale bar* = 20 μm. **b** SEM image of soil (M02) particles. Cinnabar crystals (*Cin*) coating barite (*Bar*) and Sb oxides. *Scale bar* = 10 μm

**Table 5** Elemental data from electron microprobe analyses of pyrite from the Valle del azogue mineralization

| Sample | Total | Fe | Hg | S | Sb | Ni | Co | As |
|---|---|---|---|---|---|---|---|---|
| 1 | 100.47 | 46.18 | 0.22 | 52.42 | 0.45 | 0.00 | 0.04 | 1.15 |
| 2 | 100.25 | 45.78 | 0.12 | 52.95 | 0.12 | 0.03 | 0.10 | 1.16 |
| 3 | 99.78 | 45.36 | 0.23 | 52.16 | 0.43 | 0.02 | 0.05 | 1.53 |
| 4 | 99.68 | 45.76 | 0.21 | 52.63 | 0.33 | 0.05 | 0.09 | 0.61 |
| 5 | 99.59 | 45.95 | 0.14 | 52.78 | 0.14 | 0.00 | 0.07 | 0.51 |
| 6 | 99.72 | 46.03 | 0.09 | 52.90 | 0.09 | 0.00 | 0.08 | 0.53 |
| 7 | 99.77 | 45.35 | 0.40 | 52.77 | 0.38 | 0.06 | 0.09 | 0.73 |
| 8 | 100.09 | 45.38 | 0.30 | 51.91 | 1.30 | 0.03 | 0.07 | 1.10 |
| 9 | 100.26 | 45.90 | 0.14 | 52.38 | 0.66 | 0.04 | 0.02 | 1.12 |
| 10 | 99.12 | 45.12 | 0.59 | 52.06 | 0.61 | 0.06 | 0.08 | 0.60 |
| 11 | 93.62 | 42.70 | 0.88 | 47.44 | 1.60 | 0.08 | 0.06 | 0.86 |

Data in weight percent

Based on the results of thermo-desorption measurements, we conclude that most matrix-bound Hg in tailing and mine wastes results from the recondensation of Hg (0) during the roasting process. The high Hg (0) concentration found in soil gas (Navarro et al. 2000) may also be attributed to desorption of matrix bound Hg (0). Ore samples showed a dominant cinnabar speciation (Fig. 6).

## Column experiments

The column experiments (Fig. 7) showed a decrease in As, Hg and $SO_4$ concentrations at the beginning of the experiment, from 358 μg $l^{-1}$, 67 μg $l^{-1}$ and 299 mg $l^{-1}$, down to 15.7 μg $l^{-1}$ of As, 3.4 μg $l^{-1}$ of Hg and 80.1 mg $l^{-1}$ of $SO_4$, respectively, after 210 min. The concentration of Hg at the beginning of the experiment was 67 μg $l^{-1}$, a value that approximately coincides with the result obtained from the equation relating the dissolved metallic Hg (0) and the temperature (Glew and Hames 1971):

$$\log \mathrm{Hg}\ (0) = \frac{-118.04 + 4715.2}{T + 42.03 \log T}$$

which allows a concentration of Hg (0) = 59.3 μg $l^{-1}$ at 25°C, indicating the possible presence of Hg dissolved as metallic Hg (0). The Hg concentration of leachates obtained in the leaching experiments ranged from 3.4 to 66.9 μg $l^{-1}$ and were similar to Hg concentrations of leachates in calcine samples from the Humboldt River Basin (Gray 2003).

The evolution of As content suggests that its origin is related to the dissolution of realgar (AsS) and orpiment ($As_2S_3$). Sulphate concentration is related to the presence of gypsum as a secondary phase in the soil and to the presence of sulphate originating from the oxidation of sulphides. The presence of other dissolved constituents, such as Ca, Mg, Na, K, Al, Cu (0.2–0.05 mg $l^{-1}$), Pb, Zn (8.6–1.0 mg $l^{-1}$) and Cl, could be related to the dissolution of secondary phases originating during sulphide weathering. The high pH measured during the experiment (pH = 7.54–7.91) was probably caused by the dissolution of carbonates and certain sulphates. The high concentrations of Cu and Zn can be associated with the high solubility of secondary minerals that contain these elements, such as calcantite and melanterite (Navarro et al. 2004).

Based on the mineralogical and chemical characterization of the soil sample used in the column leaching (M02), we propose in the inverse modelling a set of precipitation–dissolution reactions that might explain the mobilization of Hg (0) and the other dissolved constituents (Tables 6, 7). We also added the following chemical reactions related to Hg dissolution for evaluating the mobilization of Hg in the aqueous phase because they were not added to the "minteq" database or because the equilibrium constants were inaccurate (Morel et al. 1998; Ravichandran et al. 1998):

1. Dissolution of cinnabar

$$\mathrm{HgS} + \mathrm{H_2O} = \mathrm{Hg} + \mathrm{HS^-} + \mathrm{H^+} + 0.5\,\mathrm{O_2}\ (\log k = -52.4).$$

2.Dissolution of metallic Hg

$$\mathrm{Hg\ (liquid)} = \mathrm{Hg\ (dissolved)}\ (\log k = -6.5).$$

**Table 6** Hydrogeochemical data used in the inverse modelling

| Parameter | Input solution | Lixiviate SM1 |
|---|---|---|
| pH | 7.0 | 7.54 |
| Pe | 4.44 | 1.95 |
| Ca | 38.2 | 136.0 |
| Mg | 3.36 | 46.4 |
| Na | 13.5 | 61.1 |
| K | 1.06 | 4.01 |
| $SO_4$ | 10.3 | 299.0 |
| Cl | 7.35 | 95.4 |
| $HCO_3$ | 129.2 | 178.36 |
| $O_2$ | 8.59 | 2.73 |
| As | 0.003 | 0.34 |
| Fe | 0.001 | 1.67 |
| Hg | 0.000 | 0.067 |

Data in mg $l^{-1}$, except pH and Pe

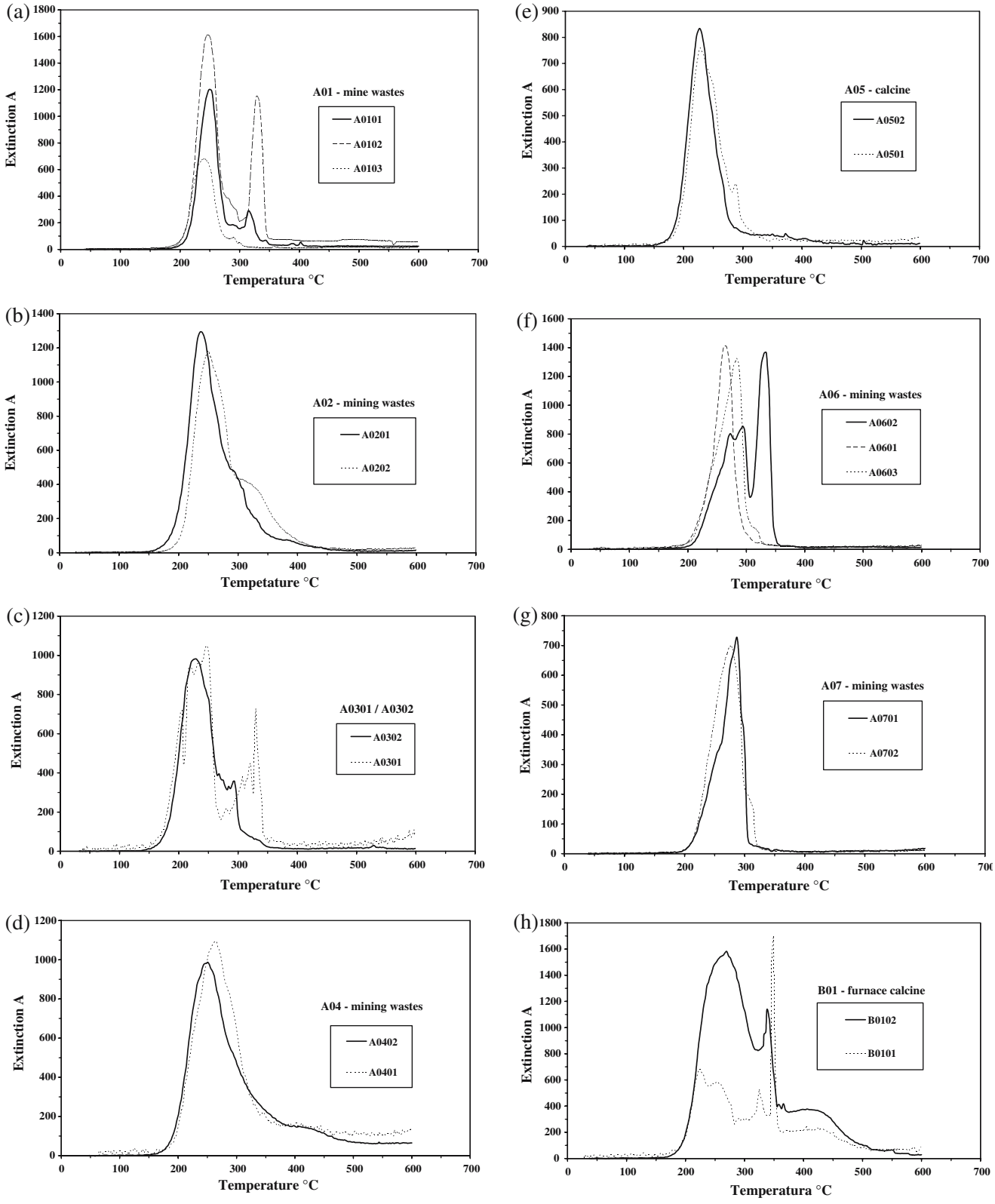


**Fig. 5** Mercury thermo-desorption curves of mine waste (**a**, **b**), soil (**c**), tailings (**d**, **f**, **g**) and calcine (**e**, **h**)

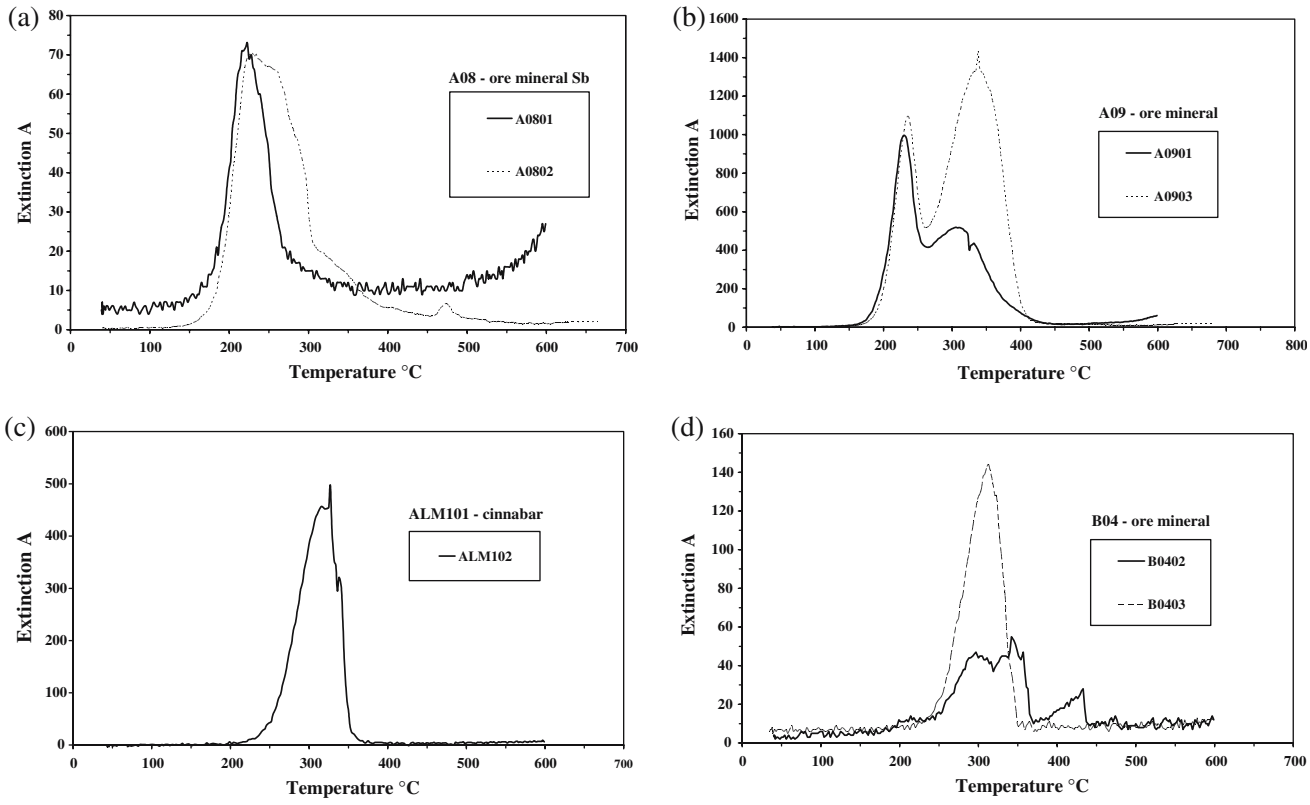


**Fig. 6** Mercury thermo-desorption curves of Sb rich ore (**a**), Hg ore (**b**), Almadén cinnabar ore (**c**), and carbonated-hosted cinnabar ore of Bayarque mine (**d**)

We used calcite, dolomite, jarosite, natrojarosite, halite, pyrite, gypsum, realgar, orpiment, cinnabar and metallic Hg as mineral phases intervening in the inverse modelling. The main mineral reactions and the equilibrium constants are shown in Table 7. The results provided eight models (Table 8) that explain the dissolution of Hg, the mobilization of As and Fe and the increase in Ca, Mg, Na, K, $SO_4$ dissolved in the effluents.

Dissolution of gypsum, jarosite and natrojarosite (Table 8) could explain the increase in sulphate and Fe,

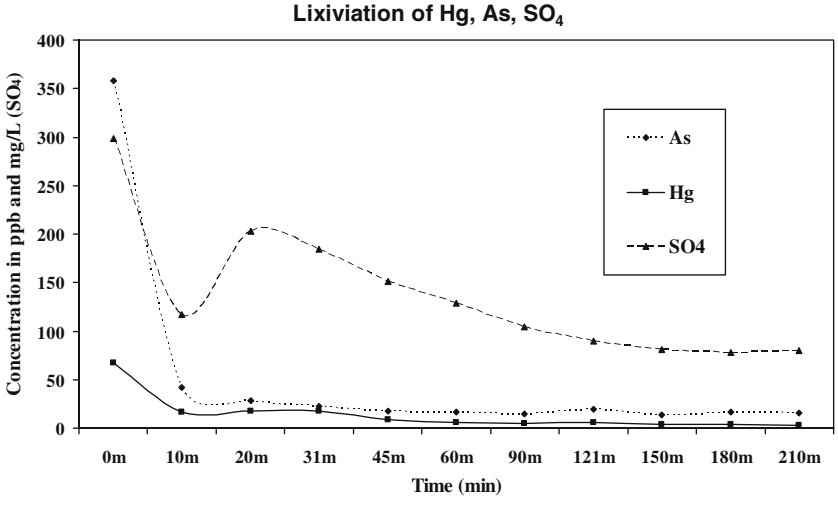


**Fig. 7** Evolution of Hg, As and $SO_4$ in the column experiment

**Table 7** Mineral phases in the inverse modelling

| Mineral phase | Reaction | log *k* (Minteq) |
|---|---|---|
| Calcite | $CaCO_3 = Ca^{2+} + 2CO_3^{2-}$ | −8.47 |
| Dolomite | $CaMg(CO_3)_2 = Ca^{2+} + Mg^{2+}\ CO_3^{2-}$ | −17.0 |
| Jarosite | $KFe_3(SO_4)_2(OH)_6 + 6H^+ = K^+ + 3Fe^{3+} + 2SO_4^{2-} + 6H_2O$ | −14.8 |
| Natrojarosite | $NaFe_3(SO_4)_2(OH)_6 + 6H^+ = Na^+ + 3Fe^{3+} + 2SO_4^{2-} + 6H_2O$ | −11.2 |
| Halite | $NaCl = Na^+ + Cl^-$ | 1.582 |
| Pyrite | $FeS_2 + 2H^+\ 2e^- = Fe^{2+} + 2SH^-$ | −18.47 |
| Gypsum | $CaSO_4{:}2H_2O = Ca^{2+} + SO_4^{2-} + 2H_2O$ | −4.848 |
| Realgar | $AsS + 3H_2O = H_3AsO_3 + HS^- + e^-$ | −19.747 |
| Orpiment | $As_2S_3 + 6H_2O = 2\ H_3AsO_3 + 3HS^- + 3H^+$ | −60.971 |

**Table 8** Models and molar transfers calculated by PHREEQC

| Phase | M-1 | M-2 | M-3 | M-4 | M-5 | M-6 | M-7 | M-8 |
|---|---|---|---|---|---|---|---|---|
| Calcite | −2.65e-003 | −2.65e-003 | −2.65e-003 | −2.65e-003 | −2.65e-003 | −2.65e-003 | −2.66e-003 | −2.66e-003 |
| Dolomite | 1.59e-003 | 1.59e-003 | 1.59e-003 | 1.59e-003 | 1.59e-003 | 1.59e-003 | 1.59e-003 | 1.59e-003 |
| Gypsum | 3.20e-003 | 3.20e-003 | 3.20e-003 | 3.20e-003 | 3.20e-003 | 3.20e-003 | 3.20e-003 | 3.20e-003 |
| Jarosite-K | 7.55e-005 | 7.55e-005 | 7.55e-005 | 7.55e-005 | 7.55e-005 | 7.55e-005 | 7.55e-005 | 7.55e-005 |
| Halite | 2.21e-003 | 2.21e-003 | 2.21e-003 | 2.21e-003 | 2.21e-003 | 2.21e-003 | 2.21e-003 | 2.21e-003 |
| Pyrite | 4.43e-005 | 4.81e-005 | 4.43e-005 | 4.79e-005 | 4.43e-005 | 4.43e-005 | 4.95e-005 | 4.93e-005 |
| Jarosite-Na | −8.04e-005 | −8.16e-005 | −8.04e-005 | −8.14e-005 | −8.04e-005 | −8.04e-005 | −8.20e-005 | −8.19e-005 |
| Realgar | | | −1.05e-005 | | −1.11e-005 | 4.50e-006 | 4.50e-006 | 4.50e-006 |
| Oripment | 2.25e-006 | 2.25e-006 | 7.50e-006 | 2.25e-006 | 7.83e-006 | | | |
| Cinnabar | 5.58e-006 | | 3.34e-007 | 3.34e-007 | | 7.83e-006 | | |
| Hg metal | −5.25e-006 | 3.34e-007 | | | 3.34e-007 | −7.50e-006 | 3.34e-007 | 3.34e-007 |

Negative values indicate precipitation and positive values dissolution

while dissolution of realgar and orpiment might cause the mobilization of As into the leachates. Moreover, the dissolution of Hg (liquid), cinnabar, dolomite, gypsum, jarosite, halite, pyrite, realgar and orpiment may account for the mobilization of contaminants (Hg and As) as well as other elements, such as Ca, Mg, Fe, Na and K. In accordance with this, Bigham and Nordstrom (2000) and Navarro et al. (2004) indicated that "the fast dissolution" of accumulated soluble salts during subsequent rainfall events may release acidity and produce "pulses" of contaminants in the environment.

Thus, when pore water migrates through the column, metallic Hg is dissolved and metals and cations are released through sulphide oxidation reactions and initially immobilized. Besides, in a semiarid environment, metals and cations can be removed from precipitated secondary mineral (jarosite, gypsum, orpiment) by dissolution–desorption mechanisms. Therefore, the dissolution of metallic Hg and secondary minerals could explain the mobility of Hg, As, Ca, Fe, Mg, Na and K in the elution experiment.

The dissolution of cinnabar, which inverse modelling results show to be theoretically possible, is sometimes inhibited by divalent cations such as $Ca^{2+}$ (Ravichandran et al. 1998) and could explain the preferential dissolution of metallic Hg in the column experiment. Moreover, based on the kinetics of cinnabar dissolution, we discard the release of large amounts of Hg (Craw et al. 2000), particularly under the prevailing environmental conditions in the Valle del Azogue mine and the leaching column experiment.

The pH–Eh conditions during the laboratory experiments (pH = 7.0–7.91, Eh = 0.115–0.135 V, $O_2$ = 2.73–8.59 mg $l^{-1}$), were in keeping with the Eh–pH equilibrium conditions for Hg species (Morel et al. 1998), indicating that the most stable species is dissolved metallic Hg (0), as is usual in aquatic environments. The column experiment showed that metals from secondary phases dissolved in pore water can be mobilized by column flow, which is very similar to what occurred in the mining site soils during wet periods. Thus, when a dry period begins, secondary phases would be newly formed at depth in soils, dumps and tailings, again producing temporary acidity and causing metal contamination accumulation.

## Conclusions

The Valle del Azogue mine provides an excellent example of mercury and arsenic contamination in soils, calcines and tailings derived from an abandoned Sb–Hg mineral deposit, that was mined in the ninetieth century and exposed to weathering in a semi-arid environment.

The primary mineralization consists of stibnite, sphalerite, siderite, chalcopyrite, pyrite quartz, calcite

and baryte. Secondary minerals, formed after weathering, include cinnabar, orpiment, realgar, gypsum and Fe and As–Sb oxide and hydroxides. By carrying out EPMA and SEM-EDS studies, we confirmed that cinnabar is a secondary phase, precipitated after the alteration of a Hg-bearing pyrite, which may reach contents of up to 8,800 mg $kg^{-1}$ of Hg.

Soils, calcines and mine wastes have high mercury contents with mean values of 357.3, 66–470 and 530–1,000 mg $kg^{-1}$, respectively. A large amount of residual Hg, remains in calcines (66–470 mg $kg^{-1}$), above the mean values cited by Rytuba (2000) for calcined tailings from rotary furnaces (20–150 mg $kg^{-1}$) and similar to calcined tailings from Scott furnaces (500–1,000 mg $kg^{-1}$) and tailings from the Idrija mercury mine (42–1,640 mg $kg^{-1}$, Biester et al. 1999).

The thermal analysis of soil and waste samples indicated that Hg was released at two different temperature ranges: 220–250 and 310–330°C. The first temperature range could correspond to metallic Hg released from the matrix, whereas the second peak, at higher temperatures, would indicate the presence of cinnabar.

In calcine samples, the metallic Hg can be attributed to Hg readsorbed after the roasting process, with a minor atmospheric deposition of Hg (0) derived from roasting plant emissions.

The results of leaching column experiments on soil sample M02, showed a decrease in As, Hg and $SO_4$ concentrations at the beginning of the experiment from 358 μg $l^{-1}$, 67 μg $l^{-1}$ and 299 mg $l^{-1}$, respectively, down to 15.7 μg $l^{-1}$, 3.4 μg $l^{-1}$ and 80.1 mg $l^{-1}$, after 210 min. These results suggest the dissolution of Hg (0) present in the soil sample, the dissolution of As from pyrite, realgar and orpiment and the mobilization of sulphates originated in the sulphide oxidation and/or the dissolution of some sulphates from the secondary phases.

The different models resulting from the inverse modelling applied to the leaching fluids, indicate that dissolution of Hg (liquid), cinnabar, dolomite, gypsum, jarosite, halite, pyrite, realgar and orpiment may account for the mobilization of Hg and As and other elements such as Ca, Mg, Fe, Na and K. The dissolution of metallic Hg in the column experiment suggests the possibility of aqueous mobilization of this contaminant in the environmental conditions of the Valle del Azogue mine.

The decrease in Hg content in soil profiles is consistent with the assumed weathering of Hg-enriched pyrite. The Hg content in soils is higher near the topographic surface where the Hg-bearing minerals (pyrite) are more exposed to the atmosphere.

**Acknowledgements** This work was supported by Spanish Ministry of Science and Technology (project REN2003-09247-C04-03) in collaboration with the Research Centre for Energy Environment and Technology (CIEMAT). The authors wish to thank Dr. M. Viladevall and the anonymous reviewer for their interesting suggestions. The authors gratefully acknowledge the leaching experiments carried out by the staff of the Department of Fluid Mechanics (UPC).

## References

Barnett MO, Harris LA, Turner RR, Stevenson RJ, Henson TJ, Melton RC, Hoffman DP (1997) Formation of mercuric sulfide in soil. Environ Sci Technol 31:3037–3043

Becker GF (1888) Geology of the Quicksilver deposits of the Pacific Slope with an Atlas. US Geological Survey Library, Document 23442, Spanish localities, pp 27–32

Biester H, Scholz E (1997) Determination of mercury phases in contaminated soils—Hg-pyrolysis versus sequential extractions. Environ Sci Technol 31:233–239

Biester H, Gosar M, Müller G (1999) Mercury speciation in tailings of the idrija mercury mine. J Geochem Explor 65:195–204

Bigham JM, Nordstrom DK (2000) Iron and aluminium hydroxysulfates from acid sulfate waters. In: Alpers CN, Jambor JL, Nordstrom DK (eds) Sulfate minerals –crystallography, geochemistry, and environmental significance. Mineralogical Society of America, Rev Miner Geochem 40:351–403

Cortazar D (1875) Reseña física y geológica de la región Norte de la provincia de Almería.- Bol. de la Comisión del Mapa Geol. España 2:164–234

Craw D, Chappell D, Reay A (2000) Environmental mercury and arsenic sources in fossil hydrothermal systems, Northland, New Zealand. Environ Geol 39(8):875–887

EPA (1991) Description and sampling of contaminated soils. A field pocket guide. EPA/625/12–91/002, 122 pp

Glew DN, Hames DA (1971) Aqueous non electrolyte solutions. Part X. Mercury solubility in water. Can J Chem 49:3114

Gray JE (2003) Leaching, transport, and methylation of mercury in and around abandoned mercury mines in the Humboldt River Basin and surrounding areas, Nevada. US Geological Survey Bull, 2210-C, 15 pp

Martínez J, Navarro A, Lunar R (1997) First reference of pyrite framboids in a Hg–Sb mineralization: the Valle del Azogue mineral deposit (SE Spain). N Jb Miner Mh Jg 4:175–184

Martínez J, Navarro A, Lunar R, García-Guinea J (1998) Mercury pollution in a large marine basin: a natural venting system in the south–west Mediterranean margin. Nat Resour 34(3):9–15

Morel FMM, Kraepiel AML, Amyot M (1998) The chemical cycle and bioaccumulation of mercury. Ann Rev Ecol Syst 29:543–566

Navarro A, Viladevall M, Font X, Rodriguez P (1994) Las mineralizaciones auríferas de Sierra Almagrera (Almería). Estudio geoquímico y modelos de yacimientos. Bol ITGE 109(2):105–112

Navarro A, Martínez J, Font X, Viladevall M (2000) Modelling of modern mercury vapor transport in an ancient hydrothermal system: environmental and geochemical implications. Appl Geochem 15:281–294

Navarro A, Collado D, Carbonell M, Sánchez JA (2004) Impact of mining activities in a semi-arid environment: Sierra Almagrera district, SE Spain. Environ Geochem Health 26:383–393

Parkhurst DL, Appelo CAJ (1999) Usefs guide to PHREEQC (version 2)—a computer program for speciation, batch-reaction, one-dimensional transport, and inverse geochemical calculations. US Geological Survey, Water-Resources Investigations Report 99–4259, 326 pp

Ravichandran M, Aiken GR, Reddy MM, Ryan JN (1998) Enhanced dissolution of Cinnabar (mercuric sulfide) by dissolved organic matter from the Florida Everglades. Environ Sci Technol 32:3305–3311

Relyea JF (1982) Theoretical and experimental considerations for the use of the column method for determining retardation factors. Radioactive Waste Manag 3(2):151–166

Rytuba JJ (2000) Mercury mine drainage and processes that control its environmental impact. Sci Total Environ 260:57–71

Rytuba JJ (2002) Mercury geoenvironmental models. In: Seal RR, Foley NK (eds) Progress on geoenvironmental models for selected mineral deposit types. US Geological Survey Open-File Report 02–195, pp 161–175

Sladek C, Gustin-Sexauer M, Kim C, Biester H (2002) Assessment of three methods for determining mercury speciation in mine wastes. Geochem Explor Environ Anal 4:369–375

Viladevall M, Font X, Navarro A (1999) Geochemical mercury survey in the Azogue Valley (Betic area, SE Spain). J Geochem Exploration 66:27–35